Soft Matter

PAPER

Investigation of the dynamical slowing down process in soft glassy colloidal suspensions: comparisons with supercooled liquids†

Debasish Saha,[a] Yogesh M. Joshi[b] and Ranjini Bandyopadhyay*[a]

The primary and secondary relaxation timescales of aging colloidal suspensions of Laponite are estimated from intensity autocorrelation functions obtained in dynamic light scattering (DLS) experiments. The dynamical slowing down of these relaxation processes are compared with observations in fragile supercooled liquids by establishing a one-to-one mapping between the waiting time since filtration of a Laponite suspension and the inverse of the temperature of a supercooled liquid that is rapidly quenched towards its glass transition temperature. New timescales associated with primary and secondary relaxation processes, such as the characteristic timescale associated with the slowdown of the secondary relaxation process and the glass transition time, are extracted to describe the phenomenon of dynamical arrest in Laponite suspensions. In results that are strongly reminiscent of those extracted from supercooled liquids approaching their glass transitions, it is demonstrated that a strong coupling exists between the primary and secondary relaxation processes of aging Laponite suspensions in the cage-forming regime. Furthermore, the experimental data presented here clearly demonstrate the self-similar nature of the aging dynamics of Laponite suspensions within a range of sample concentrations.

1 Introduction

Relaxation processes in supercooled liquids are characterised by two-step decays.[1] The faster (β) decay corresponds to the rattling of the particle within a cage formed by its neighbours, while the slower (α) decay corresponds to its cooperative diffusive dynamics between cages. The transport properties (*i.e.* viscosity, diffusivity *etc.*) and the relaxation timescales of a glass former change sharply as the glass transition is approached.[2] The primary or the α-relaxation time becomes increasingly slow and diverges in the vicinity of the glass transition. The dependence of this relaxation time on temperature in a strong glass former is nearly Arrhenius and the degree of deviation from Arrhenius behaviour is measured as 'fragility'. For fragile glass formers, the α-relaxation time shows a Vogel–Fulcher–Tammann (VFT) dependence on temperature (T), with the fragility index depending solely on the material.[3] The density of potential energy minima of the configurational states in the potential energy landscape determines the strong or fragile behaviors of supercooled liquids.[4] Strong glasses have a lower density of

minima and their entropy increases slowly with decreasing temperature, thereby resulting in nearly Arrhenius behavior.[5] In contrast, fragile glasses have a larger density of minima which causes super-Arrhenius behavior of the α-relaxation. Other secondary relaxation processes also simultaneously take place in the same temperature range. In supercooled liquids and molecular glasses, one of them is the Johari–Goldstein (JG) β-relaxation process,[6–9] which is the slowest of the secondary relaxation processes and is strongly coupled with the α-relaxation process.[10–12]

In the last two decades, colloidal glasses have emerged as excellent model candidates for the study of glasses and glass formers. While supercooled liquids can be driven towards their glass transition by rapidly quenching their temperatures, the glass transition in colloidal suspensions can be achieved by increasing the volume fraction ϕ. For a colloidal suspension of hard spheres, increasing ϕ towards a glass transition volume fraction ϕ_g plays the same role as supercooling a liquid towards its glass transition temperature T_g.[13,14]

In recent years, colloidal glasses formed by the synthetic clay Laponite have been studied extensively.[15–24] Interestingly, aging Laponite suspensions show many similarities with supercooled liquids and molecular glasses. These include the observation of well-separated fast and slow timescales,[25] the absence of thermorheological simplicity,[26,27] asymmetry in structural recovery following a step temperature change,[28,29] probe size-dependent diffusion[30] and the presence of more complex phenomena such as overaging.[31,32] Laponite particles are monodisperse discs of

[a] *Soft Condensed Matter Group, Raman Research Institute, C. V. Raman Avenue, Sadashivanagar, Bangalore 560 080, India. E-mail: debasish@rri.res.in; ranjini@rri.res.in*

[b] *Department of Chemical Engineering, Indian Institute of Technology Kanpur, Kanpur 208 016, India. E-mail: joshi@iitk.ac.in*

diameter 25 nm and width 1 nm. In an aqueous medium, the dissociation of Na^+ ions from the Laponite platelet results in negatively charged faces, while the edge of the platelet acquires a charge that depends on the pH of the medium. At a pH of 10, the edge of the Laponite platelet is estimated to have a weak positive charge.[33] Overall, in an aqueous medium, Laponite particles interact *via* face-to-face, long range repulsions and edge-to-face, short range attractions.[21] Remarkably, for $\phi > 0.004$, their aqueous suspensions undergo ergodicity breaking over a duration of days, with the free-flowing liquid getting transformed into a soft solid phase that can support its own weight.

Ruzicka *et al.* report the existence of two different concentration-dependent routes as Laponite clay suspensions approach the arrested state.[16] They claim that at high clay concentrations, the system forms a repulsive Wigner glass whose elementary units are single Laponite platelets, while at low clay concentrations (1.0 wt% < C_w < 2.0 wt%), clusters of Laponite platelets form an attractive gel. Interestingly, recent work on this subject suggests that the influence of attractive interactions cannot be ruled out even at high Laponite concentrations.[22,34] Laponite suspensions also show very interesting phase behavior as the salt concentration is varied.[35,36] A gel or a glass state, and a nematic gel state are observed at a low salt concentration as the clay concentration is increased. At very high ionic strengths, there is phase separation.[37] Recent experimental observations and simulations in the gel state show that for very high waiting times, suspensions at weight concentrations $C_w \leq$ 1.0 wt% phase separate in the absence of salt into clay-rich and clay-poor phases, while suspensions at concentrations 1.0 wt% < C_w < 2.0 wt% do not phase separate, giving rise to a true equilibrium gel obtained from an empty liquid.[38]

The ergodic-to-nonergodic transition is observed in colloidal Wigner glasses and is discussed in detail by Tanaka *et al.*[21] in the context of aging dynamics of Laponite suspensions. Two very distinct regimes of temporal change of τ_α (α-relaxation time) are observed by the authors. The initial regime, when the system is ergodic and τ_α increases exponentially with waiting time, is called the 'cage-forming' regime, while the later stage, where τ_α increases linearly with waiting time, is called the 'full-aging' regime. In the cage-forming regime, the effective volume increases with waiting time. The system gradually approaches a glass transition and finally enters the nonergodic full-aging regime. It should be noted that the aging dynamics of Laponite suspensions in the ergodic cage-forming regime is totally different from the aging of supercooled liquids just below the glass transition temperature.

In an aging Laponite clay suspension, the effective volume fraction changes spontaneously and continuously with waiting time due to the exfoliation of Laponite particles from Laponite tactoids[39] and by the simultaneous spontaneous evolution of inter-particle electrostatic interactions.[18,22,40] In this work, we perform dynamic light scattering (DLS) experiments to measure the time-evolution of the primary and secondary relaxation processes of aging Laponite suspensions in the ergodic cage-forming regime. We use our data to establish connections between aging Laponite suspensions undergoing dynamical arrest and fragile supercooled liquids approaching their glass

transitions. We show here that increasing the waiting time t_w of aging Laponite suspensions is equivalent to decreasing the thermodynamic temperature T of supercooled liquids. While the Vogel–Fulcher–Tammann (VFT) functional form (with $1/T$ mapped with sample age t_w) was demonstrated to work for the slower α-relaxation timescale of aging Laponite suspensions,[16] we show here that β-relaxation follows an Arrhenius form (with $1/T$ also mapped with sample age t_w) as expected for supercooled liquids.[9,41] A correspondence between temperature (T) and the waiting time since sample preparation (t_w) was reported in numerical studies of physical and chemical gelation[42] and in Monte Carlo simulations of patchy-particle models of Laponite discs.[38] In a recent work, the role of thermodynamic temperature in the dynamical slowing down process of a colloidal glass produced by tethering polymers to the surface of inorganic nanoparticles has been investigated in the context of soft glassy rheology.[43]

Furthermore, we demonstrate novel analogies between colloidal glasses of Laponite suspensions and supercooled liquids. We next extract new timescales (the timescale t_β^∞ associated with the fast relaxation process and the glass transition time t_g) to demonstrate several remarkable similarities that exist between supercooled liquids and soft glassy materials. We demonstrate a coupling between t_β^∞ and the glass transition time t_g. An analogous coupling between the glass transition temperature of a supercooled liquid and the activation energy corresponding to its β-relaxation process has been suggested and experimentally verified for supercooled liquids,[10–12] but has never been demonstrated in soft materials. It has been shown in the literature that the autocorrelation decay corresponding to the primary relaxation time can be successfully modeled as a stretched exponential process.[34] We show here that the stretching exponent β decreases linearly with waiting time. This observation is analogous to that in fragile supercooled liquids, where β is seen to decrease linearly with $1/T$ while approaching glass transition. This further establishes the soundness of our mapping between the waiting time of Laponite suspensions and the inverse of the temperature of supercooled liquids. Our DLS data provide indirect evidence of an exfoliation process of the nature seen earlier[39] and also demonstrate the self-similar time-evolutions of the fast and slow relaxation times, the stretching exponents β, and the width and non-Gaussian parameters (α_1 and α_2) characterizing the distributions of the slow relaxation time with changing Laponite concentration. Finally, we show that the fragility index D is concentration-independent and interpret this result in terms of the self-similar nature of the intricate potential energy landscape of aging Laponite suspensions approaching the glass transition.

2 Materials, sample preparation and experimental methods

All the experiments reported in this work are performed with Laponite RD procured from Southern Clay Products. Before every experiment, Laponite powder is dried in an oven at 120 °C for at least 16 hours. Appropriate amounts of powder are added

slowly and carefully to double-distilled and deionized Millipore water of resistivity 18.2 MΩ cm. The mixture is stirred vigorously until it becomes optically clear. The resulting suspension is filtered using a syringe pump (Fusion 400, Chemyx Inc.) at a constant flow rate (3.0 ml min^{-1}) by passing through a 0.45 μm Millipore Millex-HV syringe-driven filter unit. The filtered suspension is loaded and sealed in a cuvette for DLS experiments. Laponite suspensions of concentrations 2.0% w/v, 2.5% w/v, 3.0% w/v and 3.5% w/v are used in this study. Here, the concentration (% w/v) is the weight of Laponite in 100 ml of water. The mechanical properties of all the suspensions evolve spontaneously with time and exhibit the typical signatures of soft glassy rheology.[44]

The DLS experiments are performed with a Brookhaven Instruments Corporation (BIC) BI-200SM spectrometer equipped with a 150 mW solid state laser (NdYVO$_4$, Coherent Inc., Spectra Physics) having an emission wavelength of 532 nm. A refractive index-matching bath filled with decaline contains the cuvette filled with the sample. To avoid any kind of disturbance, the sample, once loaded, is not removed until the end of the experiment. The temperature of the bath is maintained at 25 °C by water circulation with a temperature controller (Polyscience Digital). A Brookhaven BI-9000AT Digital Autocorrelator is used to measure the intensity autocorrelation function of the light scattered from the samples. The intensity autocorrelation function $g^{(2)}(t)$ is defined as $g^{(2)}(t) = \left(\dfrac{\langle I(0)I(t)\rangle}{\langle I(0)\rangle^2} \right) = 1 + A\left|g^{(1)}(t)\right|^2$,[45] where $I(t)$ is the intensity at a delay time t, $g^{(1)}(t)$ is the normalized electric field autocorrelation function, A is the coherence factor, and the angular brackets $\langle \ \rangle$ represent an average over time. Experiments were performed at different scattering angles (60°, 75°, 90°, 105°, 120° and 135°). Data acquired at 90° are reported in the manuscript. Some representative data, acquired at 60°, are shown in the ESI.† The duration of data collection is kept long enough (2–3 minutes) to ensure a large photon count (>10^7 counts per run). Details of the data analysis protocols used in this work, for example in the calculations of the width and non-Gaussian parameters (α_1 and α_2) characterizing the distributions of the slow relaxation times, are provided in the ESI.†

3 Results and discussions

The relaxation dynamics of a medium can be analyzed by monitoring the temporal behavior of the intensity autocorrelation function $g^{(2)}(t)$. In Fig. 1, we plot the normalized intensity autocorrelation function, $C(t) = g^{(2)}(t) - 1$, for a 3.0% w/v Laponite suspension as a function of delay time, t, for experiments carried out at different waiting times t_w since filtration of the sample. $C(t)$ shows a two-step decay, suggesting the presence of two distinct relaxation timescales. In addition, the decay in the autocorrelation function slows down progressively as the sample ages. For a glassy suspension, the two-step decay of $C(t)$ can be described as a squared sum of an exponential and a stretched exponential decay given by[16]
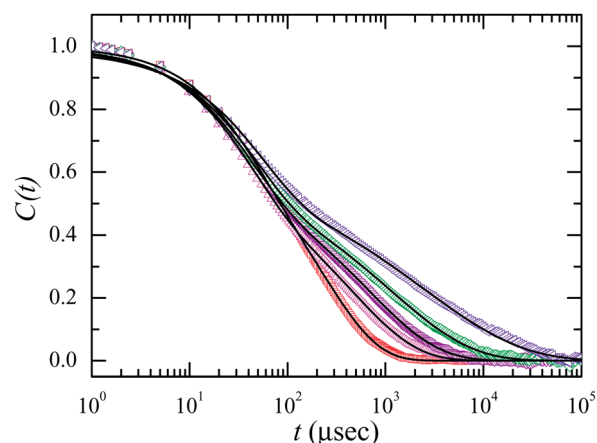

Fig. 1 The normalized intensity autocorrelation functions $C(t)$ vs. the delay time t at 25 °C and the scattering angle $\theta = 90°$ for 3.0% w/v Laponite suspension at several different waiting times t_w (from left to right): 0.5 hours (□), 6.0 hours (Δ), 9.0 hours (▽), 12.0 hours (◇) and 15.0 hours (◁). The solid lines are fits to eqn (1).

$$C(t) = [a \exp\{-t/\tau_1\} + (1 - a)\exp\{-(t/\tau_{ww})^\beta\}]^2 \qquad (1)$$

The fits to eqn (1) (shown by the solid lines in Fig. 1) describe the decays of the normalized autocorrelation functions for a range of waiting times t_w and for all the aging Laponite suspensions studied in this work. The fits are used to estimate the two relaxation timescales: τ_1, the fast relaxation timescale that is associated with the secondary relaxation process, and τ_{ww}, the slow timescale that is associated with the primary α-relaxation process. In addition, the fits also yield values of the 'stretching exponent', β, which is connected to the distribution of the α-relaxation timescales.

In Fig. 2(a), we plot the evolutions of τ_1 with increasing t_w for Laponite suspensions of different concentrations. Interestingly, τ_1 evolves in two steps. At very small t_w, τ_1 initially decreases (shown by the shaded portion in Fig. 2(a)) before increasing rapidly at large t_w. In addition, the evolution of τ_1 shifts to smaller t_w with increasing Laponite concentration.

Soon after mixing dry Laponite powder in water, hydration of clay takes place and water molecules diffuse into the inter-layer gallery causing the clusters to swell. Filtration of these suspensions breaks the clusters. After filtration, these broken clusters undergo further fragmentation.[46] In both cases, τ_1 is expected to decrease until the swelling clusters or the fragmented parts undergo dynamical arrest due to strong inter-platelet interactions that evolve spontaneously.[39] The waiting time at which τ_1 shows a minimum can therefore be considered as a measure of the time required for the onset of jamming. The waiting time associated with the minimum, $t_{w,min}$, decreases with increase in Laponite concentration (Fig. S1 in ESI†). As the Laponite concentration increases, the increase in the number of cage-forming particles can be associated with a decrease in the free space that is required for cage expansion and swelling of the clusters. The minimum in τ_1 ($t_{w,min}$) therefore shifts to smaller t_w with increase in Laponite concentration.
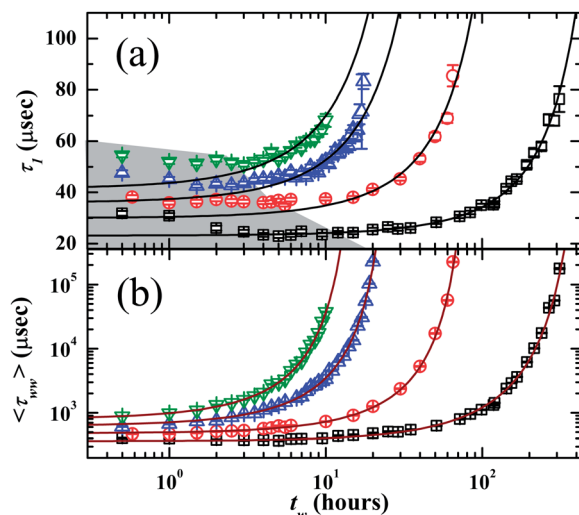
Fig. 2 (a) The fast relaxation times, τ_1 vs. waiting time t_w for Laponite samples prepared at 25 °C and at concentration 2.0% w/v ($\square$), 2.5% w/v ($\bigcirc$), 3.0% w/v ($\triangle$) and 3.5% w/v ($\triangledown$). The solid lines show fits to the modified Arrhenius functions, $\tau_1 = \tau_1^0 \exp(t_w/t_\beta^\infty)$ (eqn (2)). Data are shifted vertically for better representation. The shaded portion high-lights the initial decrease in τ_1. (b) The mean α-relaxation times, $\langle\tau_{ww}\rangle$ vs. waiting time, t_w are plotted for the same samples. The solid lines show fits to the modified VFT functions, $\langle\tau_{ww}\rangle = \langle\tau_{ww}\rangle^0 \exp(Dt_w/(t_\alpha^\infty - t_w))$ (eqn (3)).

The slow timescale τ_{ww} is identified with the α-relaxation process. The average value of τ_{ww}, $\langle\tau_{ww}\rangle = (\tau_{ww}/\beta)\Gamma(1/\beta)$, where Γ is the Euler Gamma function.[47] In Fig. 2(b), the evolution of $\langle\tau_{ww}\rangle$ is plotted as a function of t_w for different concentrations of Laponite. In contrast to the initial non-monotonic behavior of τ_1, $\langle\tau_{ww}\rangle$ remains almost constant at small t_w. At larger t_w, $\langle\tau_{ww}\rangle$ shows a sharp increase. Furthermore, the evolution of $\langle\tau_{ww}\rangle$ shifts to larger t_w with decrease in concentration of Laponite. The stretching exponents β associated with $\langle\tau_{ww}\rangle$ are obtained from fits of the data to eqn (1) and are plotted as a function of t_w in Fig. S2 of ESI.† For small values of t_w, β is close to unity. However, with increase in t_w, β decreases linearly, which signifies the broadening of the distribution associated with $\langle\tau_{ww}\rangle$. The decrease in β also shifts to smaller t_w with increase in the concentration of Laponite.

Because of self-similar curvatures in the evolutions of both τ_1 (the monotonically increasing parts) and $\langle\tau_{ww}\rangle$, the data plotted in Fig. 2 can be superposed upon horizontal and vertical shift-ing. This is shown in Fig. 3(a). The corresponding shift factors (the horizontal shift factors for τ_1 and $\langle\tau_{ww}\rangle$ are denoted by t_β^∞ and t_α^∞ respectively, and the vertical shift factors for τ_1 and $\langle\tau_{ww}\rangle$ are denoted by τ_1^0 and $\langle\tau_{ww}\rangle^0$ respectively) are plotted in Fig. 3(b). It is observed that $\langle\tau_{ww}\rangle^0$ ($\bullet$ in Fig. 3(b)) increases with Laponite concentration. This observation can be explained by considering that at higher concentrations, the particles are more easily confined in deep wells and can therefore be kinet-ically constrained at earlier times. If $q' = 1/t_\alpha^\infty$ is defined as a rate at which the system approaches the glass transition, it is seen from Fig. S3 in the ESI† that q' increases exponentially with concentration. This is connected to our observation that Laponite particles are trapped in progressively deeper energy
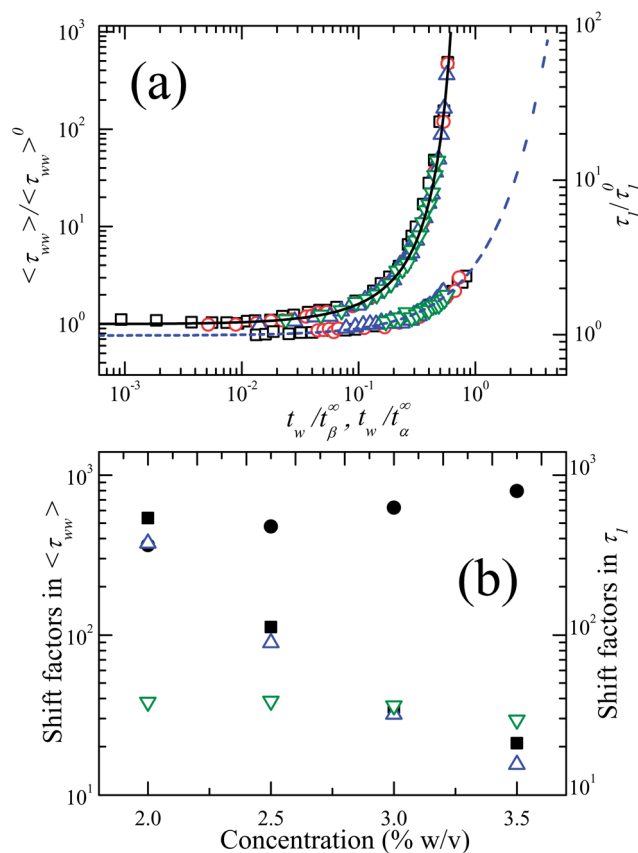

Fig. 3 In (a), superpositions of normalized τ_1 and normalized $\langle\tau_{ww}\rangle$ when plotted vs. t_w/t_β^∞ and t_w/t_α^∞, respectively, for 2.0% w/v ($\square$), 2.5% w/v ($\bigcirc$), 3.0% w/v ($\triangle$) and 3.5% w/v ($\triangledown$) Laponite suspensions. Dashed and solid lines are fits of normalized τ_1 and normalized $\langle\tau_{ww}\rangle$ to the modified Arrhenius and modified VFT functions (eqn (2) and (3)) respectively. In (b), the shift factors are plotted vs. Laponite concen-tration. The horizontal shift factors t_β^∞ (hours) and t_α^∞ (hours), corre-sponding to the fast and slow relaxation processes respectively, are denoted by $\triangle$ and $\blacksquare$, respectively. The vertical shift factors, τ_1^0 (μs) and $\langle\tau_{ww}\rangle^0$ (μs), are denoted by $\triangledown$ and $\bullet$ respectively.

wells as the Laponite concentration is increased. This confirms that the sluggishness of the α-relaxation process increases with increasing Laponite concentration. In addition to τ_1 and τ_{ww}, β also shows superposition after appropriate shifting through a vertical shift factor (V) obtained as the value of β at $t_w/t_\alpha^\infty \to 0$. This is shown in Fig. 4. The self-similarity and sharp enhance-ment of τ_1 and $\langle\tau_{ww}\rangle$ with increase in t_w are reminiscent of the changes that are observed in the fast (β) and slow (α) timescales of supercooled liquids that are quenched rapidly towards their glass transition temperatures T_g.[1,41] In supercooled liquids, the fast relaxation shows an Arrhenius dependence on temperature T given by $\tau_1 = \tau_1^0 \exp(E/k_B T)$. Here, τ_1^0 is the fast relaxation time when $T \to \infty$, E is the depth of the energy well associated with particle motion within the cage and k_B is the Boltzmann constant. The slow α-relaxation time, which represents the timescale associated with cage diffusion in supercooled liquids, demonstrates a dependence on temperature T that is given by the Vogel–Fulcher–Tammann (VFT) law: $\langle\tau_{ww}\rangle = \langle\tau_{ww}\rangle^0 \exp(DT_0/(T - T_0))$. Here, the temperature T_0 at which $\langle\tau_{ww}\rangle$ diverges is
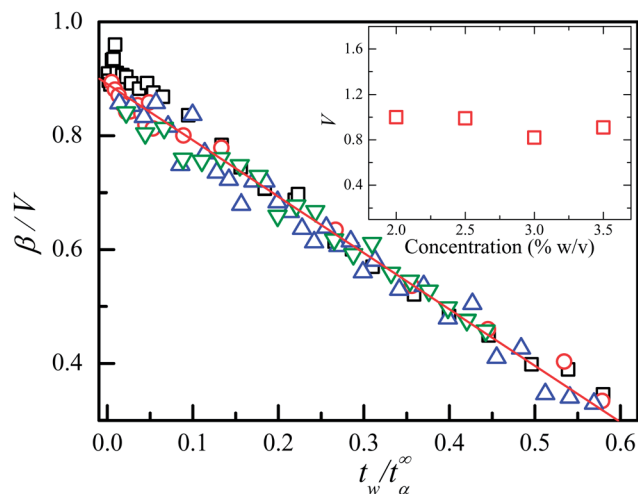
Fig. 4 Superposition of the normalized stretching coefficients β when plotted vs. t_w/t_α^∞ for 2.0% w/v ($\square$), 2.5% w/v ($\circ$), 3.0% w/v ($\triangle$) and 3.5% w/v (∇) Laponite suspensions. The straight line is a linear fit. In the inset: vertical shift factor (V) vs. Laponite concentration.

called the Vogel temperature and D is the fragility of the material. The Arrhenius equation is, therefore, a special case of the VFT equation in the limit $T_0 \to 0$.[48] Clearly, for nonzero values of T_0, the slow timescale $\langle\tau_{ww}\rangle$ diverges more rapidly than the fast timescale τ_1. In Fig. 3(a), we see a very similar situation, wherein $\langle\tau_{ww}\rangle$ diverges much more rapidly when compared to τ_1. It can therefore be appreciated that the slowdown observed in aqueous Laponite suspensions is equivalent to that seen in supercooled liquids, with the inverse of the temperature $(1/T)$ in the latter case mapped with the waiting time (t_w) in the former. In order to assess the validity of the proposed mapping, we write a modified Arrhenius equation:

$$\tau_1 = \tau_1^0 \exp(t_w/t_\beta^\infty) \qquad (2)$$

here, t_β^∞ is a characteristic timescale associated with the slowdown of the fast relaxation process. Similarly, the modified VFT equation for the mean α-relaxation time is written as:

$$\langle\tau_{ww}\rangle = \langle\tau_{ww}\rangle^0 \exp(Dt_w/(t_\alpha^\infty - t_w)), \qquad (3)$$

where t_α^∞ is identified as a Vogel time and $\langle\tau_{ww}\rangle$ is calculated from the distribution of slow relaxation times $\rho_{ww}(\tau)$ which is obtained by inverting the stretched exponential part of the autocorrelation decay. The expression for $\rho_{ww}(\tau)$ is given by,[47]

$$\rho_{ww}(\tau) = -\frac{\tau_{ww}}{\pi\tau^2}\sum_{k=0}^{\infty}\frac{(-1)^k}{k!}\sin(\pi\beta k)\Gamma(\beta k+1)\left(\frac{\tau}{\tau_{ww}}\right)^{\beta k+1} \qquad (4)$$

In eqn (2) and (3), the inverse of temperature $1/T$ in the Arrhenius and the VFT forms for supercooled liquids is mapped with t_w and $1/T_0$ is mapped with t_α^∞. It can be seen in Fig. 2 and 3 that eqn (2) and (3) fit the time-evolution of the τ_1 and $\langle\tau_{ww}\rangle$ data extremely well.

It is to be noted that multispeckle autocorrelation decay data report an initial cage-forming regime followed by a power-law

full-aging regime.[18,49] While multispeckle spectroscopy probes the ballistic dynamics of Laponite particle rearrangements over longer timescales (10^3 to 10^5 s), the DLS data presented here probe the diffusive particle dynamics at much smaller time-scales (10^{-5} to 1 s). The robustness of the VFT-type fitting is evident from Fig. 2(b) and S4 of the ESI† and confirms recent reports.[16,35] DLS is therefore a more suitable technique than multispeckle to estimate the faster relaxation times (10^{-5} to 1 s) of Laponite suspensions in the ergodic cage-forming regime. In the present work, a linear or power-law dependence of the slow relaxation time on the suspension waiting time, such as those seen in earlier reports using multispeckle techniques,[18,49] is absent. We note here that while we have restricted our observations to the ergodic cage-forming regime only, i.e. to a regime in which the autocorrelation functions decay fully and Na$^+$ ion concentration increases with waiting time (Fig. S5 in the ESI†), the multispeckle data reported earlier predominantly probed the ballistic dynamics in the full-aging regime.

In an activated process, the dependence of a characteristic timescale on temperature is used to calculate the activation energy associated with that relaxation phenomenon. For an Arrhenius relaxation process represented by $\tau_1 = \tau_1^0\exp(E/k_BT)$, E is the activation energy and k_B is the Boltzmann constant. For a VFT relaxation process described by $\langle\tau_{ww}\rangle = \langle\tau_{ww}\rangle^0\exp(DT_0/(T - T_0))$, the apparent activation energy is given by: $E_{VFT} = k_BDT_0T^2/(T - T_0)^2$.[22,50] The activation energies associated with the modified Arrhenius and VFT processes in aging Laponite suspensions can be estimated by comparing with the corresponding relations for a supercooled liquid, with $1/T$ mapped with t_w and $1/T_0$ with t_α^∞. These calculations, the details of which are supplied in the ESI†, yield the following results:

$$E = (k_B c_1)/t_\beta^\infty \qquad (5)$$

and

$$E_{VFT} = (k_B c_2)[Dt_\alpha^\infty/(t_\alpha^\infty - t_w)^2] \qquad (6)$$

here, eqn (5) represents activation energy (E) associated with τ_1, while eqn (6) represents the apparent activation energy (E_{VFT}) associated with $\langle\tau_{ww}\rangle$. In these equations, k_B is the Boltzmann constant, D is the fragility parameter, and c_1 and c_2 are constants with dimensions [time] $\times$ [temperature]. It can be seen in the inset of Fig. S6 of the ESI† that the activation energy E associated with τ_1 is independent of t_w and shows a power-law dependence on concentration of Laponite c ($E \propto c^{5.7\pm0.3}$). E_{VFT} associated with $\langle\tau_{ww}\rangle$, on the other hand, remains constant at small $t_w (\ll t_\alpha^\infty)$, but shows a strong dependence on t_w for large t_w (Fig. S6 of the ESI†). In addition, E_{VFT} shifts to smaller waiting times with increase in concentration of Laponite. This agrees with our earlier results that Laponite suspensions of higher concentrations are driven faster towards an arrested state. Furthermore, our data imply that the evolution of the potential energy landscape with increasing t_w is governed only by the α-relaxation process. The self-similar nature of E_{VFT} with changes in Laponite concentration is apparent when the data are scaled appropriately (Fig. 5(a)). The same horizontal shift factor t_α^∞, used earlier to superpose the $\langle\tau_{ww}\rangle$ data, is also used here.
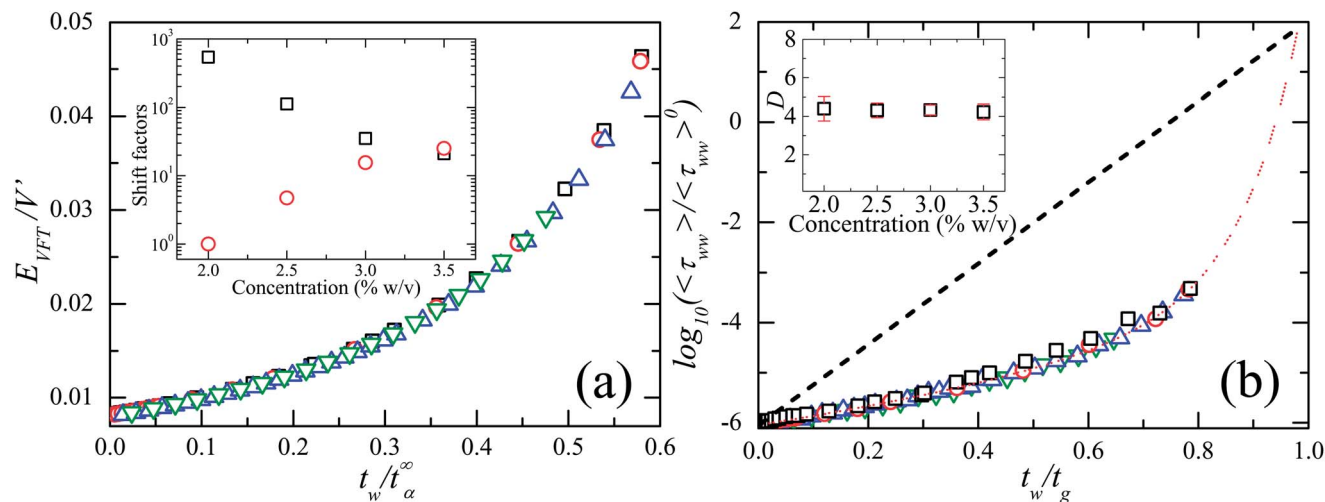
Fig. 5 (a). Superposition of the normalized apparent activation energies (E_{VFT}) associated with the α-relaxation processes as a function of (t_w/t_α^∞) for 2.0% w/v ($\square$), 2.5% w/v ($\bigcirc$), 3.0% w/v ($\triangle$) and 3.5% w/v ($\triangledown$) Laponite suspensions. Inset shows the horizontal (t_α^∞ denoted by $\square$) and vertical (V' denoted by $\bigcirc$) shift factors *vs.* Laponite concentration. (b) Angell plot for 2.0% w/v ($\square$), 2.5% w/v ($\bigcirc$), 3.0% w/v ($\triangle$) and 3.5% w/v ($\triangledown$) Laponite suspensions. The dashed diagonal straight line is the Angell plot for strong supercooled liquids, while the dotted curve is for a fragile glass former. In the inset, fragility index (D) is plotted *vs.* concentration of Laponite suspensions.

Following the definition proposed by Angell for supercooled liquids, we define the glass transition time t_g as the time since sample preparation at which $\langle \tau_{ww} \rangle = 100$ seconds for each Laponite concentration.[3] The Angell plot corresponding to the α-process of Laponite suspensions is shown in Fig. 5(b). Our data show the same behaviour expected for fragile supercooled liquids (shown by the dotted line, where $1/T$ is mapped with t_w as discussed in eqn (2) and (3)). The straight dashed line corresponds to strong glass formers for which the α-relaxation timescale shows Arrhenius behavior. We identify the constant parameter D in eqn (3) as the fragility index.[3,51,52] It is observed that the value of D remains almost constant over the Laponite concentration range explored here (inset of Fig. 5(b)). It has been pointed out that caged particles can get trapped in deeper energy wells with increase in the concentration of a glass former.[53] However, our observation that D is independent of Laponite concentration suggests that the overall topology of the potential energy landscape of aging Laponite suspensions remains unchanged even when Laponite concentration is changed.[41]

The simultaneous enhancements of the fast and slow timescales at high t_w suggest the possibility that both these processes are strongly correlated with each other. In Fig. 6, the timescale t_β^∞ associated with the fast relaxation process and obtained from fits to eqn (2) is plotted *vs.* the glass transition time t_g. It is observed that these two timescales are strongly coupled. A linear fit to the data (solid line in Fig. 6) yields $t_\beta^\infty = (1.10 \pm 0.05)t_g$. For supercooled liquids, the activation energy associated with the β-relaxation process was demonstrated to be proportional to the glass transition temperature T_g, with the exact relationship being given by $E_\beta = (24 \pm 3)RT_g$, where R is the universal gas constant.[10–12] The fast relaxation process in Laponite glasses has previously been identified as a β-relaxation process.[25] The coupling between t_β^∞ and t_g seen in Fig. 6 is not
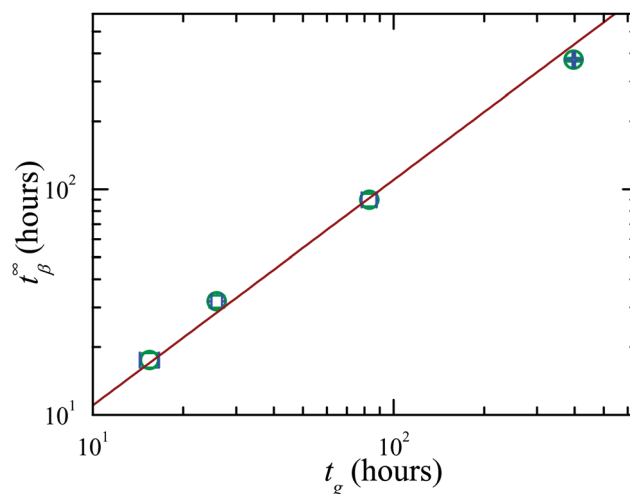

Fig. 6 The fast relaxation timescale t_β^∞ *vs.* the glass transition time t_g (from left to right - 3.5% w/v, 3.0% w/v, 2.5% w/v and 2.0% w/v). The solid line ($t_\beta^\infty \approx (1.10 \pm 0.05)t_g$) is a linear fit passing through origin.

new in the context of relaxation dynamics in supercooled liquids. The Johari–Goldstein (JG) β-relaxation seen in supercooled liquids, for example, is seen to be coupled with the α-relaxation.[9–12] Using ultrasound attenuation spectroscopy, Ali *et al.* demonstrated the fragmentation of Laponite tactoids comprising more than one Laponite platelet, in addition to the slow absorption of one or two layers of water by these tactoids.[39] Both these processes contribute to an increase in the effective volume fraction and can result in the observed slowdown of the fast relaxation process. We would like to point out here that the fragmentation of clusters into smaller entities is verfied by the DLS results reported here (shaded region in Fig 2(a)). Both the relaxation processes reported here therefore slow
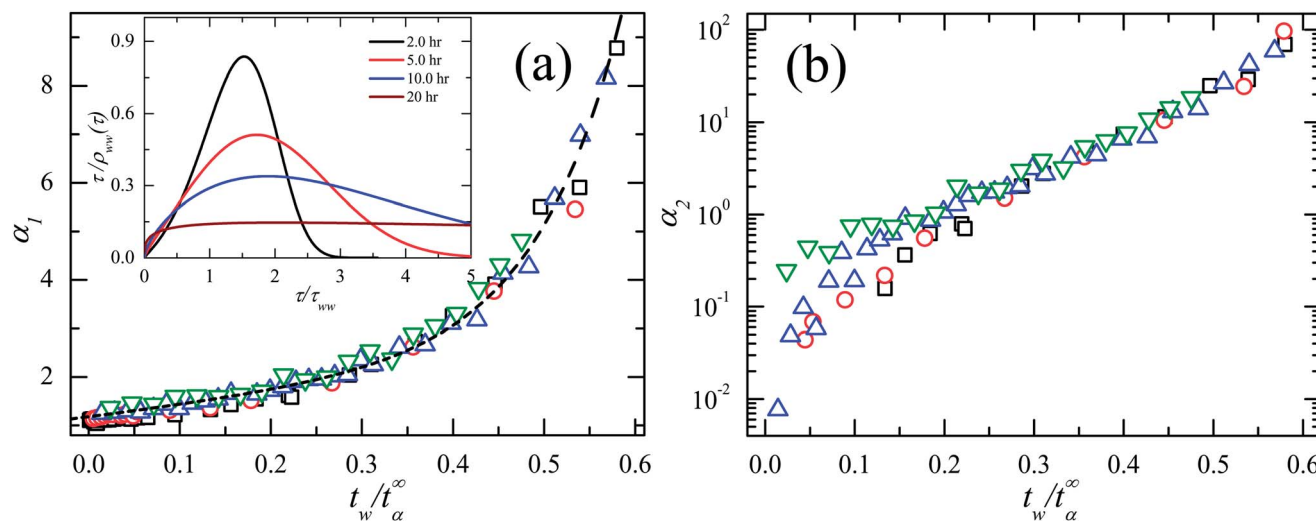
Fig. 7 (a) Width parameter α_1 $vs.$ t_w/t_α^∞ for 2.0% w/v ($\square$), 2.5% w/v ($\bigcirc$), 3.0% w/v ($\triangle$) and 3.5% w/v ($\triangledown$) Laponite suspensions. In the inset: distributions of the α-relaxation timescales plotted for 3.0% w/v Laponite suspension at 2 h, 5 h, 10 h and 20 h (from top to bottom). (b) The non-Gaussian parameter α_2 $vs.$ t_w/t_α^∞ for 2.0% w/v ($\square$), 2.5% w/v ($\bigcirc$), 3.0% w/v ($\triangle$) and 3.5% w/v ($\triangledown$) Laponite suspensions.

down due to an increase in effective volume fraction, thus explaining the observed coupling between them.

The linear decrease of β with t_w (Fig. 4 and S2 in ESI†) as the Laponite suspensions approach the glass transition is similar to the observation in fragile supercooled liquids (such as o-terphenyl mixtures[54]) where β decreases linearly with $1/T$ while approaching its glass transition. This shows that the mapping between the waiting time of a Laponite suspension in the cage-forming regime and the inverse of the temperature of a supercooled liquid is valid even though the mechanism by which the glass transition is approached is totally different in these two cases.

We now analyze the distributions of the α-relaxation timescales for various Laponite concentrations. The distributions of the α-relaxation timescales for a 3.0% w/v Laponite suspension, $\rho_{ww}(\tau)$, at four different t_w values (2 h, 5 h, 10 h and 20 h) are estimated using eqn (4) and are plotted in the inset of Fig. 7(a). In all the samples studied, the distributions broaden significantly with increasing waiting time t_w. We define a width parameter α_1 as a measure of the broadening of $\rho_{ww}(\tau)$. The values of α_1 calculated by us (details of the calculation of α_1 and Table T2† of our estimates of α_1 values are supplied in ESI†) are seen to superpose when plotted $vs.$ t_w/t_α^∞ for all the Laponite concentrations in Fig. 7(a).

We next calculate the non-Gaussian parameter α_2 (details of the calculations of α_2 and Table T3† of calculated values are supplied in ESI†) associated with the distribution of the α-relaxation timescales $\rho_{ww}(\tau)$. In Fig. 7(b), α_2 when plotted $vs.$ t_w/t_α^∞ is seen to superpose for all four Laponite concentrations. It is seen that α_2 is very small when t_w is small. However, α_2 increases sharply at higher t_w for all four Laponite concentrations. In all the superpositions presented here, it is observed that the horizontal shift factor t_α^∞ decreases rapidly with increasing Laponite concentration (Fig. 3(b) and the inset of Fig. 5(a)). The observed superpositions of α_1 and α_2, which are

achieved without any vertical shift for all the Laponite concentrations, are an additional verification of the self-similarity of the dynamic slowing down process.

4 Conclusions

In this work, we have extracted the primary and secondary relaxation timescales of aging Laponite suspensions by modeling the intensity autocorrelation functions obtained from dynamic light scattering measurements. We have compared the dynamical slowing down process of these samples with that observed in fragile supercooled liquids. While colloidal suspensions of Laponite approach the glass transition spontaneously with increasing waiting time t_w, supercooled liquids are obtained by quenching the temperature of a liquid towards its glass transition temperature at a rate that is rapid enough to avoid crystallization. It is proposed in the literature that the faster β-relaxation process of a supercooled liquid exhibits an Arrhenius temperature-dependence, while the slower α-relaxation time exhibits a VFT temperature-dependence.[1] In our work, we have demonstrated remarkably striking similarities in the relaxation processes of soft colloidal suspensions approaching dynamical arrest and fragile supercooled liquids by performing a simple one-to-one mapping between the waiting time since filtration of an aging Laponite suspension and the inverse of the thermodynamic temperature of a supercooled liquid ($t_w \leftrightarrow 1/T$).

We have identified the secondary and the primary relaxation processes of aging Laponite suspensions with, respectively, the β and the α-relaxation processes of fragile supercooled liquids. We observe here that the secondary relaxation time of aging Laponite suspensions exhibits exponential dependence on waiting times and is strongly coupled with the α-relaxation process. This kind of coupling is seen in the case of the Johari–Goldstein β-relaxation process reported in supercooled liquids

by polarization-sensitive measurements. Furthermore, we have shown that the evolutions of both the primary and secondary relaxation processes are self-similar with increasing Laponite concentration. Our estimates for the apparent activation energy corresponding to the α-relaxation process, the widths of the distributions of the α-relaxation timescales and the non-Gaussian parameters characterizing these distributions also confirm the self-similar dynamics of Laponite suspensions with increasing Laponite concentrations.

A simple relation is known to exist between the glass transition temperature T_g and energy scale E (the activation energy corresponding to the β relaxation process) of supercooled liquids. In this work, we have calculated the glass transition time t_g,[3] and have defined a new timescale corresponding to the secondary relaxation process, t_β^∞ to characterize the dynamical slowing down process in Laponite suspensions. We demonstrate the existence of a relationship between these timescales that is strongly reminiscent of the relationship that was established between the characteristic temperature/energy scales of supercooled liquids approaching their glass transitions.

A comparison of our data with the results obtained for suspensions of hard spheres near the glass transition shows that a suspension of Laponite platelets evolves in the same way with increasing waiting time (eqn (3)) as a suspension of hard spheres whose volume fraction is increased towards the random close packing fraction of $\phi_c = 0.638$.[14] The spontaneous particle exfoliation process and the inter-platelet interactions in aging Laponite suspensions evolve spontaneously with waiting time, resulting in an increase in the effective volume fraction and a simultaneous decrease in the accessible volume available to the system. This eventually leads to dynamical arrest. In the present case, the increase of the volume fraction is driven by a very complex interplay between the fragmentation/exfoliation process and the evolution of the sodium ion concentration, which results in an evolution of the inter-particle interaction. Unfortunately, the quantification of volume fractions of colloidal suspensions remains a challenging problem.[55] In hard sphere suspensions, the volume fraction plays the same role as the inverse of temperature in the glass transition of molecular glasses and supercooled liquids.[13,14] The mapping ($t_w \leftrightarrow 1/T$) established here demonstrates that aging Laponite suspensions, hard sphere glasses and fragile supercooled liquids approach their glass transitions in very similar manners, thereby confirming that aqueous suspensions of Laponite are model glass formers.

Acknowledgements

References

1 W. Gotze and S. J. Sjorgen, *Rep. Prog. Phys.*, 1992, **55**, 241–376.

2 M. D. Ediger, C. A. Angell and S. R. Nagel, *J. Phys. Chem.*, 1996, **100**, 13200–13212.

3 C. A. Angell, *J. Non-Cryst. Solids*, 1991, **131–133**, 13–31.

4 C. A. Angell, *J. Phys. Chem. Solids*, 1988, **49**, 863–871.

5 G. Adam and J. H. Gibbs, *J. Chem. Phys.*, 1965, **43**, 139–146.

6 G. P. Johari and M. Goldstein, *J. Chem. Phys.*, 1970, **53**, 2372–2388.

7 G. P. Johari and M. Goldstein, *J. Chem. Phys.*, 1971, **55**, 4245–4252.

8 M. S. Thayyil, S. Capacciolia, D. Prevostoa and K. L. Ngai, *Philos. Mag.*, 2008, **88**, 4007–4013.

9 K. L. Ngai, *J. Chem. Phys.*, 1998, **109**, 6982–6994.

10 A. Kudlik, C. Tschirwitz, S. Benkhof, T. Blochowicz and E. Rössler, *Europhys. Lett.*, 1997, **40**, 649–654.

11 A. Kudlik, C. Tschirwitz, T. Blochowicz, S. Benkhof and E. Rössler, *J. Non-Cryst. Solids*, 1998, **235**, 406–411.

12 S. Vyazovkin and I. Dranca, *Pharm. Res.*, 2006, **23**, 422–428.

13 P. N. Pusey and W. van Megen, *Nature*, 1986, **320**, 340–342.

14 L. Marshall and C. F. Zukoski, *J. Phys. Chem.*, 1990, **94**, 1164–1171.

15 D. Bonn, H. Tanaka, G. Wegdam, H. Kellay and J. Meunier, *Europhys. Lett.*, 1999, **45**, 52–57.

16 B. Ruzicka, L. Zulian and G. Ruocco, *J. Phys.: Condens. Matter*, 2004, **16**, S4993–S5002; B. Ruzicka, L. Zulian and G. Ruocco, *Phys. Rev. Lett.*, 2004, **93**, 258301.

17 B. Ruzicka and E. Zaccarelli, *Soft Matter*, 2011, **7**, 1268–1286.

18 R. Bandyopadhyay, D. Liang, H. Yardimci, D. A. Sessoms, M. A. Borthwick, S. G. J. Mochrie, J. L. Harden and R. L. Leheny, *Phys. Rev. Lett.*, 2004, **93**, 228302.

19 F. Schosseler, S. Kaloun, M. Skouri and J. P. Munch, *Phys. Rev. E: Stat., Nonlinear, Soft Matter Phys.*, 2006, **73**, 021401.

20 S. Kaloun, R. Skouri, M. Skouri, J. P. Munch and F. Schosseler, *Phys. Rev. E: Stat., Nonlinear, Soft Matter Phys.*, 2005, **72**, 011403.

21 H. Tanaka, S. Jabbari-Farouji, J. Meunier and D. Bonn, *Phys. Rev. E: Stat., Nonlinear, Soft Matter Phys.*, 2005, **71**, 021402.

22 A. Shahin and Y. M. Joshi, *Langmuir*, 2012, **28**, 15674–15686.

23 A. S. Negi and C. O. Osuji, *Phys. Rev. E: Stat., Nonlinear, Soft Matter Phys.*, 2010, **82**, 031404.

24 R. Angelini, L. Zulian, A. Fluerasu, A. Madsen, G. Ruocco and B. Ruzicka, *Soft Matter*, 2013, **9**, 10955.

25 B. Abou, D. Bonn and J. Meunier, *Phys. Rev. E: Stat., Nonlinear, Soft Matter Phys.*, 2001, **64**, 021510.

26 A. Shahin and Y. M. Joshi, *Phys. Rev. Lett.*, 2011, **106**, 038302.

27 L. C. E. Struik, *Physical aging in amorphous polymers and other materials*, Elsevier, Houston, 1978.

28 T. P. Dhavale, S. Jatav and Y. M. Joshi, *Soft Matter*, 2013, **9**, 7751–7756.

29 A. J. Kovacs, *J. Polym. Sci.*, 1956, **30**, 131–147.

30 D. R. Strachan, G. C. Kalur and S. R. Raghavan, *Phys. Rev. E: Stat., Nonlinear, Soft Matter Phys.*, 2006, **73**, 041509.

31 D. J. Lacks and M. J. Osborne, *Phys. Rev. Lett.*, 2004, **93**, 255501.

32 R. Bandyopadhyay, P. H. Mohan and Y. M. Joshi, *Soft Matter*, 2010, **6**, 1462–1466.

33 S. L. Tawari, D. L. Koch and C. Cohen, *J. Colloid Interface Sci.*, 2001, **240**, 54–66.

34 B. Ruzicka, L. Zulian, E. Zaccarelli, R. Angelini, M. Sztucki, A. Moussaid and G. Ruocco, *Phys. Rev. Lett.*, 2010, **104**, 085701.

35 B. Ruzicka, L. Zulian and G. Ruocco, *Langmuir*, 2006, **22**, 1106–1111.

36 B. Ruzicka, L. Zulian and G. Ruocco, *Philos. Mag.*, 2007, **87**, 449–458.

37 H. Tanaka, J. Meunier and D. Bonn, *Phys. Rev. E: Stat., Nonlinear, Soft Matter Phys.*, 2004, **69**, 031404.

38 B. Ruzicka, E. Zaccarelli, L. Zulian, R. Angelini, M. Sztucki, A. Moussad, T. Narayanan and F. Sciortino, *Nat. Mater.*, 2011, **10**, 56–60.

39 S. Ali and R. Bandyopadhyay, *Langmuir*, 2013, **29**, 12663–12669.

40 R. Bandyopadhyay, D. Liang, J. L. Harden and R. L. Leheny, *Solid State Commun.*, 2006, **139**, 589–598.

41 F. H. Stillinger, *Science*, 1995, **267**, 1935–1939.

42 F. Sciortino, C. D. Michele, S. Corezzi, J. Russo, E. Zaccarelli and P. Tartaglia, *Soft Matter*, 2009, **5**, 2571–2575.

43 P. Agarwal, S. Srivastava and L. A. Archer, *Phys. Rev. Lett.*, 2011, **107**, 268302.

44 K. Miyazaki, H. M. Wyss, D. A. Weitz and D. R. Reichman, *Europhys. Lett.*, 2006, **75**, 915–921.

45 B. J. Berne and R. Pecora, *Dynamic light scattering: With applications to Chemistry, Biology, and Physics*, John Wiley & Sons, New York, 1975, pp. 12–18.

46 Y. M. Joshi, *J. Chem. Phys.*, 2007, **127**, 081102.

47 C. P. Lindsey and G. D. Patterson, *J. Chem. Phys.*, 1980, **73**, 3348–3357.

48 R. G. Larson, *The structure and rheology of complex fluids*, Clarendon Press, Oxford, 1999.

49 M. Bellour, A. Knaebel, J. L. Harden, F. Lequeux and J. P. Munch, *Phys. Rev. E: Stat., Nonlinear, Soft Matter Phys.*, 2003, **67**, 031405.

50 M. T. Shaw and W. J. MacKnight, *Introduction to polymer viscoelasticity*, Wiley-Interscience, John Wiley & Sons, 2005, vol. 205, p. 271.

51 S. Sastry, *Nature*, 2001, **409**, 164–167.

52 P. G. Debenedetti and F. H. Stillinger, *Nature*, 2001, **410**, 259–267.

53 M. Goldstein, *J. Chem. Phys.*, 1969, **51**, 3728.

54 P. K. Dixon and S. R. Nagel, *Phys. Rev. Lett.*, 1988, **61**, 341–344.

55 W. C. K. Poon, E. R. Weeks and C. P. Royall, *Soft Matter*, 2012, **8**, 21–30.